Complementary relationship between daily evaporation in the environment and pan evaporation

David M. Kahler[1,2] and Wilfried Brutsaert[1]

Received 31 August 2005; revised 8 January 2006; accepted 24 January 2006; published 10 May 2006.

[1] Daily actual evaporation observed locally is compared to daily pan evaporation to clarify and test the validity of the complementary relationship at this timescale. For this purpose, use was made of actual evaporation measurements at two sites, namely, in the Konza Prairie, Kansas, during the First International Satellite Land Surface Climatology Project (ISLSCP) Field Experiment, and in the Little Washita River Basin, Oklahoma, as part of the Atmospheric Radiation Measurement Program. The corresponding pan evaporation data were obtained from nearby class A pan stations. The results of the analyses confirm the complementary relationship at this shorter timescale and lead to a procedure to estimate actual landscape evaporation by means of net radiation and pan evaporation data; they also provide support for the notion that even under conditions of decreasing incoming radiation, a negative trend in pan evaporation may still indicate a positive trend in landscape evapotranspiration.

Citation: Kahler, D. M., and W. Brutsaert (2006), Complementary relationship between daily evaporation in the environment and pan evaporation, *Water Resour. Res.*, *42*, W05413, doi:10.1029/2005WR004541.

1. Introduction

[2] In spite of rapid advances in recent years, the measurement of evaporation from the Earth's surface into the atmosphere remains a difficult task. One of the simpler and older techniques derives a measure of the evaporation from a natural surface on the basis of the measurement of the evaporation of water from a pan. In the United States, evaporation pans probably started to come into wider use in the Southwest in the late 19th century [e.g., *Carpenter*, 1891] to estimate evaporation from lakes and reservoirs [e.g., *Rohwer*, 1931; *Kohler*, 1954], and also irrigation requirements of crops in the field [e.g., *Pruitt*, 1966]. The instrument consists typically of an open container with water in it, which is allowed to freely evaporate; specific designs vary. The operator measures the amount of water that evaporates from the pan in a given time. Since evaporation occurs relatively slowly and nearly imperceptibly, measurements are usually taken on a daily basis. The class A pan is the official network instrument developed by the U.S. Weather Bureau [e.g., *Kadel and Abbe*, 1916], but it has been used in many other countries as well.

[3] The basic idea in the deployment of evaporation pans was that these measurements can be assumed to be proportional to actual evaporation of moist surfaces, such as lakes or irrigated fields. Because pans of various designs have produced data for many regions throughout the world over the years, attempts have also been made to use these data to estimate actual evaporation even in nonmoist environments. However, as pan evaporation measurements were never intended for this purpose, this has remained an elusive goal. In fact, there still exists confusion about the proper interpretation of the available measurements. This was brought out recently in the context of global change studies. Starting with *Peterson et al.* [1995], numerous studies have reported observations of decreasing pan evaporation over large areas in different regions throughout the world over the past 50 years. Although these decreases were not universal, they appear to be widespread enough to indicate a general trend. Initially, these pan evaporation trends were interpreted as an indication of a decreasing trend in terrestrial evaporation. However, this interpretation contrasts with the reported general increases in global precipitation in the same period [e.g., *Diaz et al.*, 1989; *Karl et al.*, 1996; *Dai et al.*, 1997; *Karl and Knight*, 1998], which would suggest an increasing rate of evaporation. It also contrasts with subsequent reports of increases in actual evaporation estimated by water budget methods over large areas where pan evaporation had been decreasing [e.g., *Milly and Dunne*, 2001; *Walter et al.*, 2004]; in these approaches annual evaporation was obtained as the difference between annual precipitation and river outflow from a basin.

[4] These seemingly opposing trends were at first referred to as the evaporation paradox by *Brutsaert and Parlange* [1998], who suggested that its resolution may lie in the complementary relationship. In the context of pan evaporation, this complementary relationship [*Bouchet*, 1963] indicates that pan evaporation and actual evaporation should diverge from each other when the land dries; thus *Brutsaert and Parlange* [1998] suggested that a decrease in pan evaporation could signal an increase in actual evaporation. This interpretation of the pan evaporation trends has been gaining some acceptance [e.g., *Lawrimore and Peterson*, 2000; *Golubev et al.*, 2001; *Hobbins et al.*, 2004]. However, it was also received with considerable skepticism in other studies [*Cohen et al.*, 2002; *Roderick and Farquhar*, 2002; *Ohmura and Wild*, 2002; *Liu et al.*, 2004], in which it was

[1]School of Civil and Environmental Engineering, Cornell University, Ithaca, New York, USA.

[2]Now at Department of Civil and Environmental Engineering, Duke University, Durham, North Carolina, USA.

0043-1397/06/2005WR004541

argued that the decreasing pan evaporation is the result of decreasing solar irradiance, or global dimming, and therefore an indicator of decreasing landscape evaporation.

[5] These conflicting interpretations underscore the fact that the relationship between evaporation from a pan and evaporation from the surrounding landscape, and specifically their complementary behavior, are still poorly understood. The main objective of this study is to elucidate this issue. Different implementations of the complementary principle have been tested experimentally in a number of studies, some of them [e.g., *Giusti*, 1978; *Hobbins et al.*, 2004] using pan evaporation to represent apparent potential evaporation. However, this has mostly been done with annual or other long-term evaporation data, often obtained with water budget studies over entire river basins. Temporal and spatial averaging and other similar filtering operations tend to reduce the information content of physical data. A second, equally serious problem is that the use of data, time averaged over periods of weeks or months, with mass transfer formulations based on turbulence theory, can lead to marked systematic error in surface flux calculations [e.g., *Brutsaert*, 1982, p. 207]. Thus, to unravel some of the underlying physical mechanisms, this must be avoided and it is crucial to work with local observations and to reduce the timescale to the shortest possible one, namely, the daily value in the case of pan evaporation data. Accordingly, in this study daily actual evaporation observed locally is compared to daily pan evaporation to clarify and test the validity of the complementary relationship at this timescale. Two sites were selected that contain the instrumentation to measure the necessary variables: the Konza Prairie in Kansas and the Little Washita River Basin in Oklahoma. In addition, on the basis of this analysis, a procedure is proposed to derive actual landscape evaporation by means of net radiation and pan evaporation data.

2. Advection-Aridity Approach With Pan Evaporation

[6] *Bouchet* [1963] appears to have been the first to promulgate the complementary concept formally in general terms. However, in its original formulation, it was not clear how the different variables should or could be estimated or measured. This may explain, in part, why it took some time before the concept was being understood and accepted, and why over time several different interpretations have been proposed in the literature on how it should be applied in practice. The specific derivation of the extended version of the concept for the present study is implicit in the earlier work of *Brutsaert and Stricker* [1979], *Brutsaert and Parlange* [1998], and *Brutsaert* [2005] and can be summarized as follows.

[7] When a natural surface, uniformly covered with active vegetation, is amply supplied with moisture, the actual evaporation taking place from it is said to be the potential evaporation E_{po}. Under such conditions the evaporation is generally proportional to pan evaporation E_{pa}. Thus the actual evaporation from a well watered surface with adequate moisture, so that only the available energy supply is the limiting factor, satisfies $E = E_{po} = C_p E_{pa}$, in which C_p is an assumed constant of proportionality; this constant converts the evaporation from the pan to that from the surrounding vegetation under potential conditions. In any given situation the exact value of C_p depends on a number of environmental factors. As the landscape evaporation decreases from potential evaporation, for any possible reason such as a decrease in available moisture or a decrease in photosynthesis, an energy flux ΔQ, not used up in evaporation, is now liberated, or

$$L_e E_{po} - L_e E = \Delta Q, \tag{1}$$

in which L_e is the latent heat of vaporization. This energy flux ΔQ is therefore available to raise the evaporation rate from a locally moist surface, such as a pan, above the potential evaporation E_{po}. Let it be assumed that this increase in E_{pa} is directly proportional to ΔQ, so that it can be written as

$$C_p L_e E_{pa} = L_e E_{po} + b\Delta Q, \tag{2}$$

where b is the constant of proportionality. The magnitude of b is a measure of the effectiveness with which heat transfer takes place between the pan and its surroundings, in response to the change in aridity of the environment ΔQ, and relative to the response of the natural evaporation from the surrounding landscape; it can therefore be referred to as an effectiveness parameter. In Bouchet's original formulation it was assumed implicitly that $b = 1$. However, a pan in a drying environment receives more energy per unit horizontal area than the surrounding land surface because its sides and bottom are exposed and allow additional heat transfer due to radiation and conduction; moreover, a pan is also subject to local advection, so that it has a larger water vapor transfer coefficient than the surrounding surface, due to its small size [see *Brutsaert*, 1982, Figures 7.4, 7.5, and 7.8]. These two factors cause pan evaporation to be more responsive to ΔQ than the evaporation from the surrounding environment; therefore it can be expected that $b > 1$. By elimination of ΔQ between (1) into (2), one obtains the generalized complementary relationship

$$(1 + b)E_{po} = C_p E_{pa} + bE. \tag{3}$$

[8] In principle, any universal relationship can best be formulated by expressing the relevant variables in dimensionless form. Accordingly, normalization of (3) by the real potential evaporation E_{po} yields the following expressions for the scaled actual evaporation $E_+ = E/E_{po}$ and for the scaled pan evaporation $E_{pa+} = C_p E_{pa}/E_{po}$, both as functions of the dimensionless variable $E_{MI} = E/(C_p E_{pa})$,

$$E_+ = \frac{(1 + b)E_{MI}}{1 + bE_{MI}} \tag{4}$$

and

$$E_{pa+} = \frac{1 + b}{1 + bE_{MI}}. \tag{5}$$

The dimensionless variable $E_{MI} = E/(C_p E_{pa})$ indicates how close the landscape is to potential conditions, with a maximal value of $E_{MI} = 1$ for potential conditions; as a convenient reference, this ratio E_{MI} can be called the evaporative surface moisture index. Equations (4) and (5)

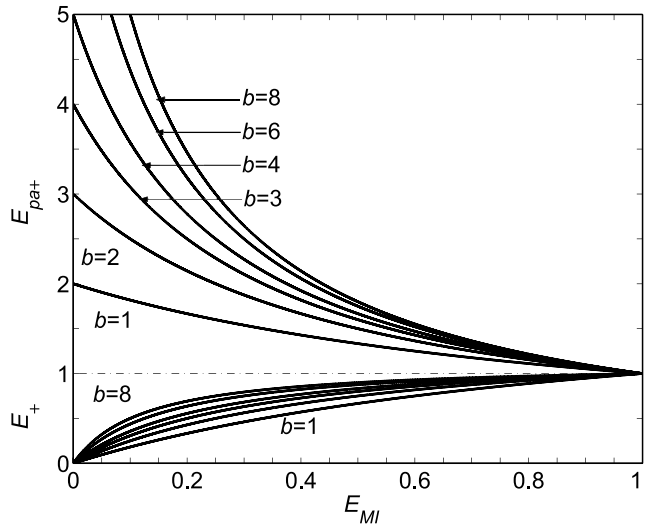

Figure 1. Scaled actual evaporation $E_+ = E/E_{po}$ and scaled pan evaporation $E_{pa+} = C_p E_{pa}/E_{po}$, as functions of the evaporative moisture index $E_{MI} = E/(C_p E_{pa})$, on the basis of the extended complementary relationship (3). The curves were obtained with (4) and (5), respectively, for different values of the effectiveness parameter, namely, for b = 1, 2, 3, 4, 6, and 8.

are displayed in Figure 1 for different values of the effectiveness parameter b. Figure 1 illustrates how pan evaporation will depart from, and exceed actual evaporation below potential conditions, as $E_{MI} < 1$. It also shows that this difference between E_{pa} and E will increase as the available surface moisture decreases.

[9] The practical application of (3), (4) and (5), to relate pan evaporation with actual evaporation from the surrounding land surface, requires a knowledge of the pan coefficient C_p, of the effectiveness parameter b and of the true potential evaporation, E_{po}. The parameters C_p and b are empirical and they can be determined from past experience or by calibration, as will be shown below. The potential evaporation E_{po} is more difficult to estimate. Indeed, it is the evaporation which would take place from the area under consideration, if conditions were potential, given the same solar radiative conditions and the same general mesoscale circulation pattern. When the surface is drying because insufficient moisture is available, it is difficult to infer the atmospheric and surface conditions that would prevail if water were not lacking, and even more difficult to estimate the evaporation under those hypothetical conditions. In the advection-aridity approach of *Brutsaert and Stricker* [1979] it was assumed that, as a close approximation, true potential evaporation can be estimated by means of *Priestley and Taylor*'s [1972] empirical extension of equilibrium evaporation to describe evaporation from a wet surface under conditions of minimal advection. With this assumption one can write for the present purpose

$$E_{po} = \alpha_e \frac{\Delta}{\Delta + \gamma}(R_n - G), \tag{6}$$

in which $\Delta \equiv de^*/dT$ is the slope of the saturation water vapor pressure at the temperature of the air, γ is the psychometric constant, R_n is the net radiation, G is the heat flux into the ground, and α_e is an empirical constant. The value of α_e is typically of the order of 1.2 to 1.3, but for natural surfaces it can cover a wide range from 1.0 to 1.5 [e.g., *Chen and Brutsaert*, 1995; *Brutsaert and Chen*, 1995]; therefore in practical applications it is best determined experimentally for any given surface. The rationale for the use of (6) lies in the fact that it is fairly robust, in that the calculated result depends mainly on the solar radiation input, and much less on temperature and humidity. Indeed, as the environment dries, and conditions depart from potential, with the same solar radiation input, the surface and air temperature are likely to increase on account of ΔQ in (1). However, with increasing surface temperature and decreasing atmospheric humidity, $(R_n - G)$ is likely to decrease, whereas $\Delta/(\Delta + \gamma)$ is bound to increase somewhat [e.g., *Brutsaert*, 2005, Figure 4.2], thus leaving the product of these two quantities in (6) relatively unchanged.

3. Experimental Settings and Data

[10] The analysis was carried out with experimental data observed at two venues, namely, an area in the Flint Hills region in northeastern Kansas, and an area in the watershed of the Little Washita River in Oklahoma.

3.1. Konza Prairie Research Natural Area

[11] This area, also referred to as Konza Prairie, is among the more rugged sections of a much larger region consisting of similar topography and vegetation; located in the Flint Hills near Manhattan, Kansas, it is owned by the Nature Conservancy and operated by Kansas State University. It was home to the First International Satellite Land Surface Climatology Project (ISLSCP) Field Experiment (FIFE), which took place in the summers of 1987 and 1989 and whose objectives are described by *Sellers et al.* [1988, 1992]. The Konza satisfied all of FIFE's requirements, one of which was a "strong seasonal climatic forcing." Much of the Konza is grassland and undergoes periodic controlled burns. The mean annual precipitation is 835 mm and the annual temperature range is from −2.7°C to 26.6°C [*Bark*, 1987]. The data collection consisted of a network of stations that measured many meteorological parameters.

[12] Actual evaporation used in the present study was calculated by the energy budget with Bowen ratio (EBBR) technique with data taken from station 40 (39°06′35.0″N, 96°31′21.0″W) in 1987, and station 944 (39°05′46.0″N, 96°31′56.0″W) in 1989, which were operated by a team of the University of Washington. *Fritschen and Simpson* [1989] and *Fritschen et al.* [1992] provide a comprehensive description of the surface energy flux systems in place at these stations during FIFE. The U.S. Army Corps of Engineers monitors a class A evaporation pan nearby the Konza (39°14′51.0″N, 96°35′57.0″W). The pan's location is some 16.7 km away at a bearing of 337° from station 40, and 17.9 km away from station 944 at a bearing of 341°. The City of Manhattan and the Kansas River lie between the pan and the two EBBR stations, but far enough not to be the source of local advection. The pan is situated in a mowed, unirrigated field at the Tuttle Creek Reservoir, directly south some 300 m from the dam. To avoid moist air advection effects from the reservoir, days with a predominantly

northerly wind were removed from the data set. Average daily wind direction was calculated by a daily weighted average of the wind direction. To implement a simple modular arithmetic system, the cosine of the wind direction was taken by means of $\bar{w}_d = \sum_{day} w_s \cos(w_d) / \sum_{day} w_s$, in which w_s is the wind speed, w_d is the wind direction averaged every 30 min, and $\bar{w}_d$ is the average daily wind direction index, which indicates a predominantly northerly wind when it has a value larger than zero.

[13] The data of the FIFE experiment were obtained from the FIFE Information System (FIS) compiled at Goddard Space Flight Center and available from Oak Ridge National Laboratory (http://www-eosdis.ornl.gov/FIFE/FIFE_Home.html). The FIFE surface flux data were reevaluated in 1992 by the investigators. The newer data were used in this study. The data at the two FIFE stations included among others latent heat flux (W/m^2), net radiation (W/m^2), ground heat flux (W/m^2), soil moisture (%), air temperature (K), relative humidity (%), wind direction (°), and wind speed (m/s). The pan evaporation and precipitation data for the pan station near the Tuttle Creek Reservoir were obtained from the National Climatic Data Center (NCDC) through the Climate Data Inventory (http://lwf.ncdc.noaa.gov/oa/ncdc.html).

3.2. Little Washita River Basin

[14] The second site is located within the Little Washita River Basin near Chickasha, Oklahoma. This basin which covers roughly 610 km^2 has been the subject of hydrologic studies for the past 35 years by the Agricultural Research Service of the U.S. Department of Agriculture. The terrain is gently rolling and fairly typical for the southern Great Plains; the land use is mainly rangeland, pasture and cropland, with some isolated patches of forest. The general characteristics of this region are described by *Schiebe et al.* [1993]. The watershed receives an average of 747 mm of annual precipitation with relatively dry summers; for example, July receives an average of 56 mm.

[15] A major installation of the Atmospheric Radiation Measurement (ARM) Program, run by the United States Department of Energy, Office of Biological and Environmental Research, Environmental Sciences Division, is the Southern Great Plains (SGP) site, which straddles Kansas and Oklahoma [e.g., *Stokes and Schwartz*, 1994]. Among the many facilities distributed over the SGP site is a remote station located just outside Cement, Oklahoma (34°57′00.0″N, 98°04′33.6″W), where among other variables evaporation is measured by the EBBR method. The area around this station is well covered with dense vegetation typical of rangeland and pasture. A more thorough description of the instruments is included in the literature of the Washita '92 experiment that used this EBBR station, station 4 [*Stannard et al.*, 1993; *Kustas et al.*, 1996]. The data used in this study were measured at this station during the warm season (starting and ending when pan measurements occurred, approximately from May to September) over a period from 1993 to 2003. A class A evaporation pan is being operated by the Oklahoma State University South Central Research Station (N35°03′00.0″, W97°55′00.0″) some 18.3 km away from the EBBR station at a bearing of approximately 52°. The pan sits in an unirrigated, mowed, Bermuda grass lawn (L. Hurt, South Central Research Station, Oklahoma State University, personal communication, 2005).

[16] The data at the ARM Cement station were obtained from the ARM Data Archive at Oak Ridge National Laboratory (http://www.arm.gov). These data are similar to those recorded at the two EBBR stations at FIFE and include the latent heat flux (W/m^2), net radiation (W/m^2), ground heat flux (W/m^2), soil moisture (%), air temperature (K), relative humidity (%), wind direction (°), and wind speed (m/s). The pan evaporation and precipitation data at the South Central Research Station were also obtained from the National Climatic Data Center (NCDC) through the Climate Data Inventory (http://lwf.ncdc.noaa.gov/oa/ncdc.html).

3.3. General Data Treatment

[17] At both the FIFE and the ARM site, actual evaporation was measured continuously and reported as 30-min values. These values were averaged for each daytime period, between 0600 and 1800 hours Central Standard Time (CST). Other variables were averaged for the day. Any days missing more than 25% of their data were removed.

[18] Data were subject to review using data quality reports when available; all questionable points were removed for the analyses. Additionally, because of notorious systematic errors in the measurement of precipitation, pan evaporation data from rainy days were suspected to be systematically overestimated, and therefore were also removed.

4. Methodology, Implementation, and Results

4.1. Complementarity of Actual and Pan Evaporation?

[19] The daily values of actual evaporation E estimated using the EBBR method at the FIFE site and at the ARM site are displayed graphically in Figures 2 and 3, respectively, against the moisture index $E_{MI} = E/(C_p E_{pa})$ in which it is assumed that $C_p = 1$ (see below). Also shown in Figures 2 and 3 are the corresponding pan evaporation measurements E_{pa}. Figures 2 and 3 definitely show some degree of complementary behavior of E and E_{pa}, because large values of E_{pa} generally appear to correspond with small values of E, and vice versa. However, the relationship between the two variables is not very clear, nor very consistent, as the data appear as clouds of points with considerable scatter. The reason for this is that for the same moisture status of the surface widely different evaporation rates are possible, all depending on the atmospheric conditions.

4.2. Complementarity of the Scaled Vapor Fluxes

[20] As pointed out above, a relationship can be considered truly universal only when it can be expressed in terms of dimensionless variables. Equations (3), (4) and (5) suggest how this can be accomplished in the present case, namely, by scaling the fluxes with the true potential evaporation E_{po}.

[21] To determine E_{po} by means of (6), the following variables are needed, the air temperature T_a, the net radiation R_n, and the ground heat flux G. While the latter was measured at both sites, such measurements are often unreliable because the soil properties and the soil moisture content tend to be so highly variable over short distances;

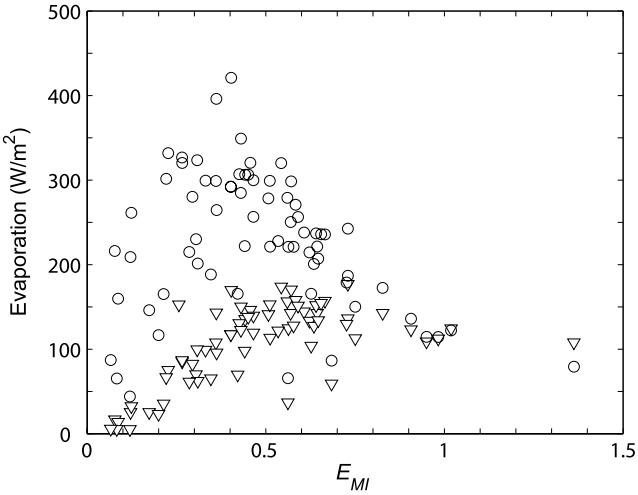

Figure 2. Actual evaporation E (triangles) and pan evaporation E_{pa} (circles) obtained from measurements in the Konza Prairie and plotted against the moisture index E_{MI} with $C_p = 1$.

moreover, both at the FIFE and at the ARM site, the G measurements were made some 15 to 20 km from the pan evaporation stations. Therefore, for the present analysis, it was decided to parameterize in terms of the net radiation, as follows:

$$G = c_R R_n, \tag{7}$$

in which c_R is an empirical constant, which typically has values of the order of 0.1 (dense grass) to 0.3 (bare soil) for hourly timescales, but smaller for daily time steps [e.g., *Brutsaert*, 2005]. With (7), the potential evaporation (6) assumes the form

$$E_{po} = \alpha_e(1 - c_R)\frac{\Delta}{\Delta + \gamma}R_n, \tag{8}$$

in which $\alpha_e(1 - c_R)$ can now be considered a single empirical constant to be determined by calibration for any given surface.

[22] Thus to apply (4) and (5) with the variables E and E_{pa} scaled by means of (8), three constants need to be determined, namely, $\alpha_e(1 - c_R)$, the effectiveness parameter b, and the pan coefficient C_p. However, the pan coefficient C_p has already been the subject of numerous intensive investigations in the past, and it can therefore be estimated from the vast amount of information available in the irrigation engineering literature [e.g., *Allen et al.*, 1998]. In practice, this coefficient is normally considered as the product of two coefficients, namely, $C_p = K_p K_c$, in which K_p converts the pan evaporation to the evaporation from short lawn grass under potential conditions, and K_c converts the evaporation from the short grass to that of the vegetation under consideration; the former is of the order of 0.8 [e.g., *Pruitt*, 1966; *Brutsaert*, 1982], whereas the latter is of the order of 1.2 in the case of crops which may be representative of rangeland vegetation under truly potential conditions, such as rice paddies, Indian corn, frequently cut alfalfa hay, cotton, wetlands, swamps and orchards with ground cover. This means that for mixed natural vegetation, it is not unreasonable to assume that C_p is not very different from unity; moreover, as can be seen in (2), the evaporative performance of the pan is also embodied in the parameter b, so that its value may compensate for any possible inaccuracies in C_p. This was tested with a few trial calculations, which showed that the overall performance of (3), (4) and (5) was not materially affected by small changes in C_p around an assumed value of one.

[23] With the value of C_p determined, the two remaining parameters were estimated as follows. First all the available evaporation data are isolated for which $E_{MI} = E/(C_p E_{pa})$ is larger than 0.95 and smaller than 1.0; it is assumed that these data represent potential conditions so that actual evaporation E can be described by (8). Thus the value of $\alpha_e(1 - c_R)$ can be determined as the average of the ratios $E/[R_n\Delta/(\Delta + \gamma)]$ of all of these days. This allows next the scaling of all the available data of E and E_{pa} by means of (8). Finally, the value of b can be estimated by a trial-and-error routine applied to (3) in the range $4 \leq b \leq 10$. For a given trial value b, the sum of the square errors is noted; the process is repeated with gradually smaller increments until the value of b is obtained which yields the smallest sum of the square errors. For the Konza the best fit was obtained with $\alpha_e(1 - c_R) = 1.13$, and $b = 4.33$. For the Little Washita, these values were $\alpha_e(1 - c_R) = 0.89$, and $b = 6.88$.

[24] The scaled daily values of actual evaporation E_+ and the corresponding scaled pan evaporation measurements E_{pa+} are displayed graphically in Figure 4 for the Konza Prairie and in Figure 5 for the Little Washita River basin; the data points in Figures 4 and 5 definitely show a more pronounced complementary behavior than their unscaled counterparts in Figures 2 and 3. Also shown in Figures 4 and 5 are the theoretical curves obtained with (4) and (5); the curves generally give a good description of these scaled latent heat fluxes. The complementarity of the data and the good agreement with the curves support the notion that with proper calibration the simplified equilibrium evaporation, as

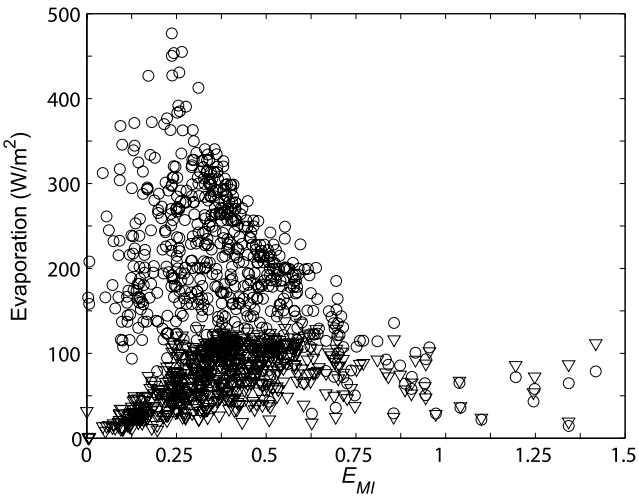

Figure 3. Actual evaporation E (triangles) and pan evaporation E_{pa} (circles) obtained from measurements in the Little Washita basin and plotted against the moisture index E_{MI} with $C_p = 1$.

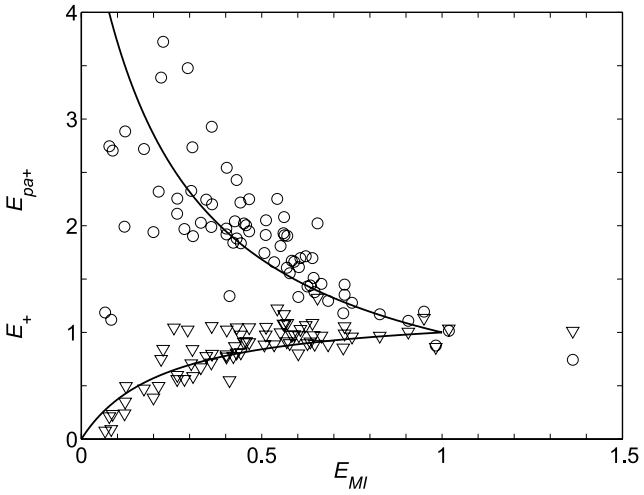

Figure 4. Same data as in Figure 2 for the Konza Prairie but normalized as $E_+ = E/E_{po}$ (triangles) and as $E_{pa+} = C_pE_{pa}/E_{po}$ (circles), in which $C_p = 1$ and the normalization is performed with the potential evaporation as obtained with (8) and $\alpha_e(1 - c_R) = 1.13$. The curves represent (4) and (5), with $b = 4.33$.

defined in (8), can serve as a robust measure of the true potential evaporation to scale E and E_{pa} in the context of the complementary concept.

4.3. Longer Timescales

[25] The analysis was also carried out with monthly averages of the variables to test the effect of timescale on the values of the parameters. However, in plotting the results in the manner of Figures 4 and 5, it was found that the monthly values fell nearly perfectly on the curves, and could not be distinguished from the daily values, except that they displayed less scatter. Therefore these results are not shown here. Similar results were obtained with the annual data for the Little Washita.

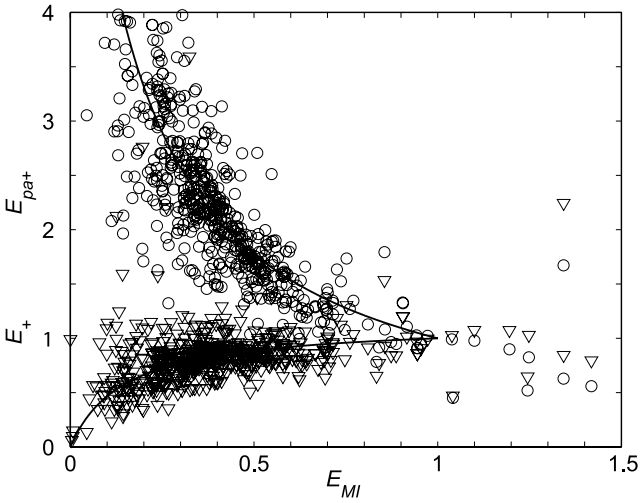

Figure 5. Same data as in Figure 3 for the Little Washita basin but normalized as $E_+ = E/E_{po}$ (triangles) and as $Ep_{a+} = C_pE_{pa}/E_{po}$ (circles), in which $C_p = 1$ and the normalization is performed with the potential evaporation as obtained with (8) and $\alpha_e(1 - c_R) = 0.89$. The curves represent (4) and (5), with $b = 6.88$.

4.4. Alternative Moisture Indices

[26] The ratio of actual evaporation to pan evaporation arises naturally as the surface moisture index $E_{MI} = E/(C_pE_{pa})$ in the derivation of (4) and (5). The use of this ratio provides strong support for the complementary relationship. One drawback of this ratio is that it involves the variables under consideration. Although this can usually not be avoided in the process of nondimensionalization, the possibility was investigated to validate the complementary relationship on the basis of some more independent moisture indices. Accordingly, the relationship between pan evaporation and actual evaporation was also tested as a function of two other measures of the moisture status of the surface, namely, the measured soil moisture content and the antecedent precipitation index of *Kohler and Linsley* [1951]. However, it was found that with the daily data of the present study neither one of these variables was able to provide a measure of the availability of the surface moisture for evaporation in the present context. Therefore these results are not shown.

5. Estimation of Evaporation From Pan Data

[27] The results of the analysis in the previous section can now be used operationally to estimate actual evaporation with data of air temperature, net radiation, and pan evaporation. This is accomplished by rearranging (3) with (8) as follows:

$$E = \alpha_e(1 - c_R)\left(\frac{1+b}{b}\right)\frac{\Delta}{\Delta+\gamma}R_n - \frac{C_p}{b}E_{pa}, \qquad (9)$$

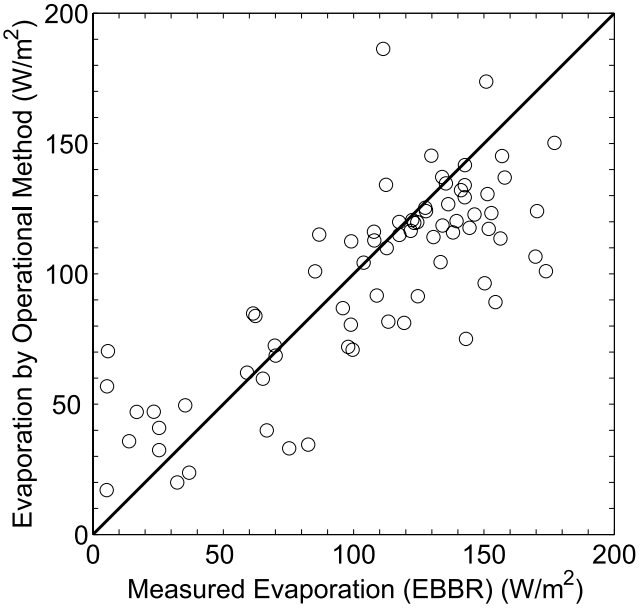

Figure 6. Comparison between daily evaporation values (W m^{-2}) measured with EBBR at the Konza Prairie and the results calculated using the operational method (9), with $C_p = 1$ and with the calibrated constants $\alpha_e(1 - c_R) = 1.13$ and $b = 4.33$.

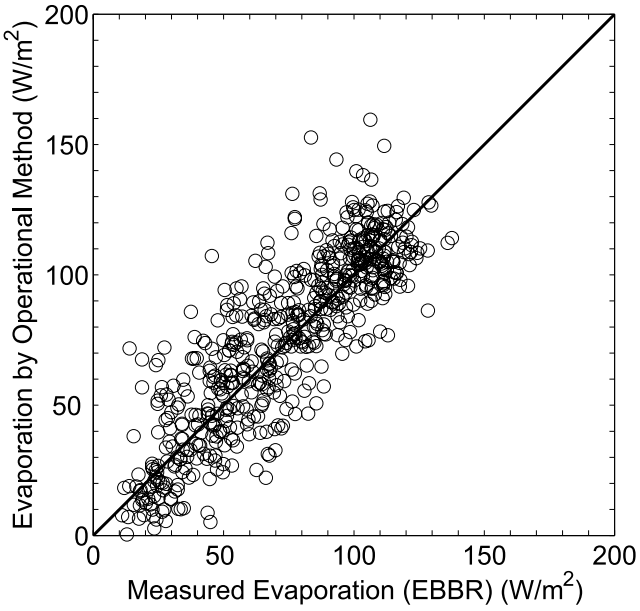

Figure 7. Comparison between daily evaporation values (W m^{-2}) measured with EBBR in the Little Washita basin and the results calculated using the operational method (9), with $C_p = 1$ and with the calibrated constants $\alpha_e(1 - c_R) = 0.89$ and $b = 6.88$.

where Δ and γ are defined behind (6), and C_p can be assumed to be one as indicated above; the variable E_{pa} is measured by an evaporation pan and R_n is the net radiation. The parameters $\alpha_e(1 - c_R)$ and b can be determined by the calibration described in the previous section. When this is not possible, typical values from the literature are available, which indicate $\alpha_e = 1.26$, $c_R = 0.15$ (dense vegetation), so that $\alpha_e(1 - c_R) = 1.07$. Values of $b = 4.3$ and 6.9 were obtained in the present study, so a value of the order of 5 may be taken as a default value until more information becomes available.

[28] The calibrated values were used to compute actual evaporation shown in Figures 6 and 7 and the typical default values were used to compute actual evaporation shown in Figures 8 and 9. Both compare evaporation modeled with (9) to actual evaporation measured by EBBR. As shown in Figure 6, actual evaporation is estimated with a standard error of S = 32.6 W/m^2 and a coefficient of determination of $R^2 = 0.62$ for the Konza Prairie and, as shown in Figure 7, with S = 18.5 W/m^2 and $R^2 = 0.74$ for the Little Washita. To test the effectiveness of the operational procedure with default parameters, both sets of data were also used to estimate actual evaporation with $\alpha_e = 1.26$, $c_R = 0.15$, and $b = 5$. The results shown in Figures 8 and 9 indicate that, as might be expected, (9) does not perform as well, yielding S = 33.2 W/m^2 and $R^2 = 0.63$ for the Konza Prairie, and S = 30.0 W/m^2 and $R^2 = 0.73$ for the Little Washita. On average, for the Konza Prairie, evaporation is underpredicted, while the opposite holds for the Little Washita. This procedure was also implemented with monthly averages as a further test of the applicability of the proposed technique for longer-term prediction. Only the data from the Little Washita basin were used for this purpose, since the available records of the FIFE experiment are too short. Figure 10 shows a comparison between the monthly values measured with EBBR and the results calculated using (9) with the monthly averages of $R_n\Delta/(\Delta + \gamma)$ and E_{pa} and the optimal values of the parameters. The calculated values indicate an improved agreement and a smaller standard error of S = 11.0 W/m^2;

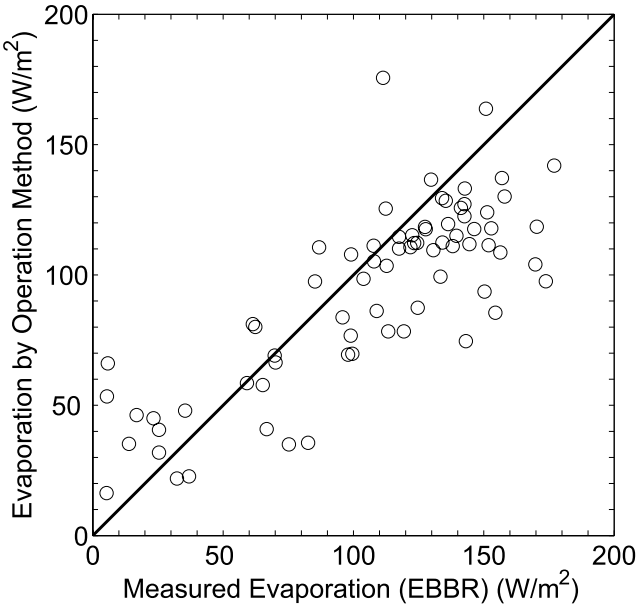

Figure 8. Comparison between daily evaporation values (W m^{-2}) measured with EBBR in the Konza Prairie and the results calculated using the operational method (9), with $C_p = 1$ and with the default values of the constants $\alpha_e(1 - c_R) = 1.07$ and $b = 5$.

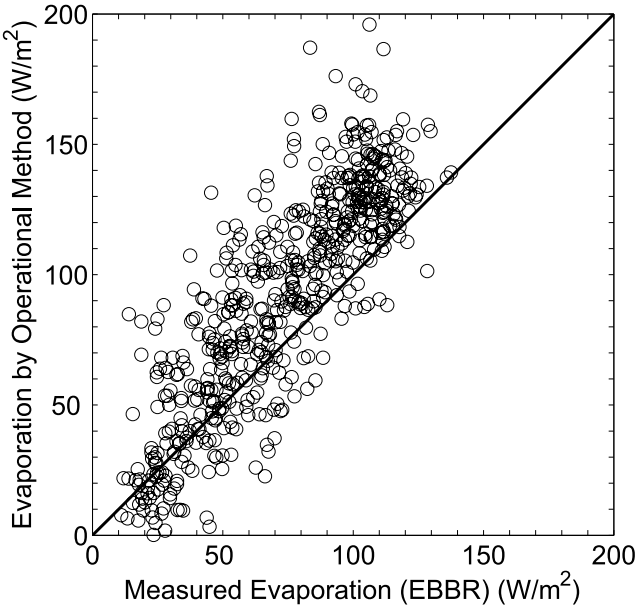

Figure 9. Comparison between daily evaporation values (W m^{-2}) measured with EBBR in the Little Washita basin and the results calculated using the operational method (9), with $C_p = 1$ and with the default values of the constants $\alpha_e(1 - c_R) = 1.07$ and $b = 5$.

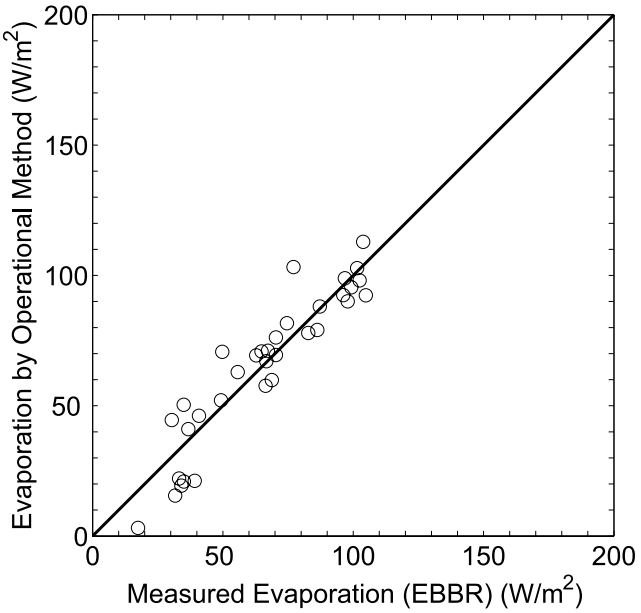

Figure 10. Comparison between monthly evaporation values (W m^{-2}) measured with EBBR in the Little Washita basin and the results calculated using the operational method (9) with $C_p = 1$ and with the calibrated constants $\alpha_e(1 - c_R) = 0.89$ and $b = 6.88$.

however, because of the smaller number of points, the coefficient of determination is only $R^2 = 0.70$.

6. Conclusions

[29] Actual daily evaporation data measured in the field at two sites, namely, at the First ISLSCP Field Experiment in the Konza Prairie, Kansas, and at the Atmospheric Radiation Measurement Program in the Little Washita River Basin, Oklahoma were compared with the corresponding pan evaporation data obtained from nearby pan stations. Analysis of these data in the framework of the complementary concept has produced the following findings.

[30] At the daily timescale, distinct evidence for complementarity between actual evaporation and pan evaporation can emerge only when the data are properly scaled in order to eliminate variability induced by the vagaries of the weather and other related factors. Until now, the complementary relationship applied with pan data has mostly been tested and validated with annual and other long-term averages, in which most of the temporal variability had been filtered out. The present results provide an explanation for the fact, that in the case of short-term unscaled data the complementary features of actual evaporation and apparent potential evaporation (estimated from pan evaporation or Penman's equation) are not always very obvious and may often remain hidden.

[31] A calibrated form of the equilibrium evaporation can serve as a robust measure to scale actual evaporation and pan evaporation in the framework of the complementary relationship between them; this is a confirmation of the earlier proposal by *Brutsaert and Stricker* [1979]. The main drawback of this scale is that it is only a first-order approximation of true potential evaporation, and that its main calibration parameter, viz. Priestley and Taylor's α_e was found, herein and in other studies, to vary somewhat depending on atmospheric conditions and from one location to another. When no other information is available, its default value $\alpha_e = 1.26$ may only be used as a rough estimate.

[32] The inclusion of the effectiveness parameter allows Bouchet's original concept to be extended and applied with pan evaporation and other small evaporation surfaces in a dry environment. This parameter, denoted as b herein, reflects the effectiveness of the heat transfer between a pan and its surroundings, in response to a change in aridity ΔQ, and in comparison with the response of the natural landscape evaporation. It was hypothesized after Bouchet to be close to unity in previous implementations of the complementary concept; in contrast, the present study has shown that it is in fact considerably larger and that values around $b \approx 5$ may be more appropriate. Although the results may be fairly insensitive to its exact value, ideally it should be determined by calibration. The reason for these relatively large values of b observed in this study is that a pan in a drying environment is subject to more heat transfer than the surrounding land surface; the sides and bottom of the pan are exposed to additional radiation and conduction and its small size creates local advection, which results in a larger heat transfer coefficient. These effects cause the pan to be a very responsive and sensitive instrument, such that a small change in energy released by a decreasing landscape evaporation may produce a fivefold to sixfold increase in pan evaporation. In other words, the pan is much more sensitive to changes in aridity than the landscape evaporation itself.

[33] With the inclusion of this parameter the advection-aridity approach provides a formulation that can give a good description of the experimental data. Conversely, as expressed in (9), the approach was shown to predict actual evaporation with fair accuracy on the basis of measurements of pan evaporation in conjunction with measurements of air temperature and net radiation. This newly investigated parameter b, and its variability, call for further studies into its physical significance pertaining to energy transport within the small scales studied here. Finally, the proposed formulation also shows how, even under conditions of decreasing net radiation, a negative trend in pan evaporation may still be indicative of a positive trend in landscape evaporation; the experimental validation of this formulation provides further support for the earlier assertion of *Brutsaert and Parlange* [1998].

[34] In the present study the land surface moisture status was characterized by the moisture index $E_{MI} = E/(C_p E_{pa})$. While other indices, such as more direct measures of the soil water content, and antecedent precipitation indices, have been used in the past for this purpose, in the present study with daily data these indices were found to be unsuitable. Water storage in the soil and the health of the vegetation have characteristic timescales of the order of weeks [e.g., *Chen and Brutsaert*, 1995]; evidently, they cannot properly characterize the often rapidly varying evaporative conditions in the field at the daily timescale.

References

Allen, R. G., L. S. Pereira, D. Raes, and M. Smith (1998), Crop evapotranspiration: Guidelines for computing crop water requirements, *FAO Irrig. Drain. Pap. 56*, Food and Agric. Org. of the U. N., Rome.

Bark, D. (1987), Konza Prairie Research Natural Area, in *The Climates of the Long-Term Ecological Research Sites*, edited by D. Greenland, *Occas. Pap. 44*, pp. 45–50, Inst. of Arctic and Alp. Res., Univ. of Colo., Boulder.

Bouchet, R. J. (1963), Evapotranspiration reelle, evapotranspiration potentielle, et production agricole, *Ann. Agron.*, *14*, 543–824.

Brutsaert, W. (1982), *Evaporation into the Atmosphere: Theory, History and Applications*, 299 pp., Springer, New York.

Brutsaert, W. (2005), *Hydrology*: *An Introduction*, 605 pp., Cambridge Univ. Press, New York.

Brutsaert, W., and D. Chen (1995), Desorption and the two stages of drying of natural tallgrass prairie, *Water Resour. Res.*, *31*, 1305–1313.

Brutsaert, W., and M. B. Parlange (1998), Hydrologic cycle explains the evaporation paradox, *Nature*, *396*, 30.

Brutsaert, W., and H. Stricker (1979), An advection-aridity approach to estimate actual regional evapotranspiration, *Water Resour. Res.*, *15*, 443–450.

Carpenter, L. G. (1891), Section of meteorology and irrigation engineering, fourth annual report, pp. 29–97, Agric. Exp. Station, State Agric. Coll., Fort Collins, Colo.

Chen, D., and W. Brutsaert (1995), Diagnostics of land surface spatial variability and water vapor flux, *J. Geophys. Res.*, *100*, 25,595–25,606.

Cohen, S., A. Ianetz, and G. Stanhill (2002), Evaporative climate changes at Bet Dagan, Israel, 1964–1998, *Agric. For. Meteorol.*, *111*, 83–91.

Dai, A., I. Y. Fung, and A. D. Del Genio (1997), Surface observed global land precipitation variations during 1900–88, *J. Clim.*, *10*, 2943–2962.

Diaz, H. F., R. S. Bradley, and J. K. Eischeid (1989), Precipitation fluctuations over global land areas since the late 1800's, *J. Geophys. Res.*, *94*, 1195–1210.

Fritschen, L. J., and J. R. Simpson (1989), Surface energy and radiation balance systems: General description and improvements, *J. Appl. Meteorol.*, *28*, 680–689.

Fritschen, L. J., E. T. Kanemasu, D. Nie, E. A. Smith, J. B. Stewart, S. B. Verma, and M. L. Wesely (1992), Comparisons of surface flux measurement systems used in FIFE 1989, *J. Geophys. Res.*, *97*, 18,697–18,713.

Giusti, E. (1978), Hydrology of the karst of Puerto Rico, *U.S. Geol. Surv. Prof. Pap. 1012*.

Golubev, V. S., J. H. Lawrimore, P. Y. Groisman, N. A. Speranskaya, S. A. Zhuravin, M. J. Menne, T. C. Peterson, and R. W. Malone (2001), Evaporation changes over the contiguous United States and the former USSR: A reassessment, *Geophys. Res. Lett.*, *28*, 2665–2668.

Hobbins, M. T., J. A. Ramírez, and T. C. Brown (2004), Trends in pan evaporation and actual evapotranspiration across the conterminous U.S.: Paradoxical or complementary?, *Geophys. Res. Lett.*, *31*, L13503, doi:10.1029/2004GL019846.

Kadel, B. C., and C. Abbe Jr. (1916), Current evaporation observations by the Weather Bureau, *Mon. Weather Rev.*, *44*, 674–677.

Karl, T. R., and R. W. Knight (1998), Secular trends of precipitation amount, frequency, and intensity in the USA, *Bull. Am. Meteorol. Soc.*, *79*, 231–241.

Karl, T. R., R. W. Knight, D. R. Easterling, and R. G. Quayle (1996), Indices of climate change for the United States, *Bull. Am. Meteorol. Soc.*, *77*, 279–292.

Kohler, M. A. (1954), Lake and pan evaporation, in *Water-Loss Investigations: Lake Hefner Studies*, technical report, *U.S. Geol. Surv. Prof. Pap. 269*, pp. 127–148.

Kohler, M. A., and R. K. Linsley (1951), Predicting the runoff from storm rainfall, *Res. Pap. 34*, pp. 1–9, U.S. Weather Bur., Washington, D. C.

Kustas, W. P., D. I. Stannard, and K. J. Allwine (1996), Variability in surface energy flux partitioning during Washita '92: Resulting effects on Penman-Monteith and Priestley-Taylor parameters, *Agric. For. Meteorol.*, *82*, 171–193.

Lawrimore, J. H., and T. C. Peterson (2000), Pan evaporation in dry and humid regions of the United States, *J. Hydrometeorol.*, *1*, 543–546.

Liu, B., M. Xu, M. Henderson, and W. Gong (2004), A spatial analysis of pan evaporation trends in China, 1955–2000, *J. Geophys. Res.*, *109*, D15102, doi:10.1029/2004JD004511.

Milly, P. C. D., and K. A. Dunne (2001), Trends in evaporation and surface cooling in the Mississippi River basin, *Geophys. Res. Lett.*, *28*, 1219–1222.

Ohmura, A., and M. Wild (2002), Is the hydrologic cycle accelerating?, *Science*, *298*, 1345–1346.

Peterson, T. C., V. S. Golubev, and P. Y. Groisman (1995), Evaporation losing its strength, *Nature*, *377*, 687–688.

Priestley, C. H. B., and R. J. Taylor (1972), On the assessment of surface heat flux and evaporation using large-scale parameters, *Mon. Weather Rev.*, *100*, 81–92.

Pruitt, W. O. (1966), Empirical method of estimating evapotranspiration using primarily evaporation pans, in *Evapotranspiration and Its Role in Water Resources Management*, pp. 57–61, Am. Soc. of Agric. and Biol. Eng., St. Joseph, Mich.

Roderick, M. L., and G. D. Farquhar (2002), The cause of decreased pan evaporation over the past 50 years, *Science*, *298*, 1410–1411.

Rohwer, C. (1931), Evaporation from free water surfaces, *Tech. Bull. 271*, U.S. Dep. of Agric., Washington, D. C.

Schiebe, F. R., J. W. Naney, P. B. Allen, and T. J. Jackson (1993), Little Washita watershed, in *Hydrology Data Report, Washita '92*, edited by T. J. Jackson and F. R. Schiebe, *NAWQL 93-1*, chap. 2, U.S. Dep. of Agric., Agric. Res. Serv., Durant, Okla. (Available at http://hydrolab.arsusda.gov/washita92/datarpt.htm.).

Sellers, P. J., F. J. Hall, G. Asrar, D. E. Strebel, and R. E. Murphy (1988), The first ISLSCP field experiment (FIFE), *Bull. Am. Meteorol. Soc.*, *69*, 22–27.

Sellers, P. J., F. J. Hall, G. Asrar, D. E. Strebel, and R. E. Murphy (1992), An overview of the First International Satellite Land Surface Climatology Project (ISLSCP) Field Experiment (FIFE), *J. Geophys. Res.*, *97*, 18,345–18,371.

Stannard, D. I., W. P. Kustas, K. J. Allwine, and D. E. Anderson (1993), Micrometeorological data collection, in *Hydrology Data Report, Washita '92*, edited by T. J. Jackson and F. R. Schiebe, *NAWQL 93-1*, chap. 5, U.S. Dep. of Agric., Agric. Res. Serv., Durant, Okla. (Available at http://hydrolab.arsusda.gov/washita92/datarpt.htm.).

Stokes, G. M., and S. E. Schwartz (1994), The Atmospheric Radiation Measurement (ARM) program: Programmatic background and design of the cloud and radiation testbed, *Bull. Am. Meteorol. Soc.*, *75*, 1201–1221.

Walter, M. T., D. S. Wilks, J. Y. Parlange, and R. L. Schneider (2004), Increasing evapotranspiration from the conterminous United States, *J. Hydrometeorol.*, *5*, 405–408.

W. Brutsaert, School of Civil and Environmental Engineering, Cornell University, Ithaca, NY 14853, USA.

D. M. Kahler, Department of Civil and Environmental Engineering, Duke University, Durham, NC 27708, USA. (david.kahler@duke.edu)